

represents less than 1/5 of the time taken for the transition to occur.

The great circle pole path, the antiparallelism of the transition, and the reduced intensity are features common to many but not all of the more recent reversals which have been studied in detail<sup>9-14</sup>. The relationship between the remanent intensity of rocks and the palaeointensity of the geomagnetic field is not necessarily simple. The uniformity of the section both lithologically and magnetically suggests, however, that the coincidence of the reduced remanent intensity with the transition zone is more than accidental. The use of thermally cleaned results in this context is not critical as the uncleaned intensity profile exhibits the same major features.

These observations are relevant to a discussion of the mechanism of geomagnetic field reversal. There are two extreme possibilities: decay and subsequent antiparallel re-establishment of the dipole field, or a 180° dipole 'flip' with no change in strength. The palaeolatitude of the sampling site is 8°, and abundant halite casts offer independent evidence of a tropical climate. At such low latitudes a 'flip' reversal could give rise to a spectrum of intensity profiles ranging from no change to an increase by a factor 2, depending on the meridian followed by the pole. In the present case the transitional pole path passes close to the sampling site and an increase in intensity could therefore be expected. The clear minimum actually observed thus provides strong evidence of a real decrease in the dipole moment during the reversal.

Several workers<sup>15-17</sup> have noted that the period of reduced intensity during recent polarity transitions is longer than the time needed for the direction to reverse, although others have found that these periods coincide<sup>18</sup>. It is difficult to place this Precambrian reversal in either class but there is a suggestion of very rapid variations in intensity immediately before and after the change of direction, such as has been seen in more recent reversals<sup>19</sup>.

The term 'field excursion' or 'systematic deviation' is usually applied to short duration deviations in pole position, which are greater than 40° or 50° but significantly less than 180° and which are not immediately associated with field reversals<sup>20-22</sup>. The field excursion reported here fits this description but we stress that it is represented by a single site mean. The reduced and/or unstable intensity near the excursion supports findings<sup>21,23-25</sup> which correlate low latitude poles with reduced intensity.

Perhaps the most significant point about the field excursion is its location near the transition pole path, which suggests that, though it occurred a significant time before the reversal, it is perhaps not wholly unrelated to it. Some coincidence of great circle paths described during several separate reversals<sup>9</sup> and during distinct field excursions<sup>25</sup> has been observed in the recent palaeomagnetic record. The result reported here is consistent with these results and with the hypothesis that field excursions represent aborted reversals<sup>20</sup>. It also provides support for the existence of long lived non-dipole sources<sup>25</sup> or stable equatorial dipoles<sup>9</sup>.

Whatever is the exact mechanism involved in geomagnetic field reversals—dipole decay or dipole flip-over, or a combination of these—the data reported here indicate that the process has apparently remained essentially unchanged for nearly  $2 \times 10^9$  yr of the Earth's history. The only significant difference involves the possibility that the transition occupied a considerably longer time interval than more recent reversals<sup>8</sup>. These observations place additional limits on the history of the geomagnetic field and, by implication, the thermal evolution of the Earth's core.

This work was supported by a grant from the National Research Council of Canada. We thank Dr E. W. McMurry and Dr D. I. Gough for reading the manuscript.

D. K. BINGHAM  
M. E. EVANS

*Institute of Earth and Planetary Physics,  
University of Alberta,  
Edmonton, Alberta, Canada*

Received October 11, 1974.

- 1 Hoffman, P. F., *Geol. Surv. Pap. Can.*, 68-42 (1968).
- 2 Fahrig, W. F., and Jones, D. L., *Can. J. Earth Sci.*, 6, 679-688 (1969).
- 3 Irving, E., Park, J. K., and McGlynn, J. C., *Can. J. Earth Sci.*, 9, 744-755 (1972).
- 4 Irving, E., *Paleomagnetism and its Application to Geological and Geophysical Problems* (Wiley, New York, 1964).
- 5 Irving, E., Molyneux, L., and Runcorn, S. K., *Geophys. J. R. astr. Soc.*, 10, 451-454 (1969).
- 6 Tarling, D. H., *Geophys. J. R. astr. Soc.*, 11, 423-432 (1966).
- 7 Kukal, Z., *Geology of Recent Sediments* (Academic Press, London, 1971).
- 8 McElhinny, M. W., *Comments on Earth Sci. Geophys.*, 1, 150-158 (1971).
- 9 Creer, K. M., and Ispir, Y., *Phys. Earth planet. Interiors*, 2, 283-293 (1970).
- 10 Goldstein, M. A., Strangway, D. W., and Larson, E. E., *Earth planet. Sci. Lett.*, 7, 231-239 (1969).
- 11 Watkins, N. D., *Geophys. J. R. astr. Soc.*, 17, 121-149 (1969).
- 12 Van Zijl, J. S. V., Graham, K. W. T., and Hales, A. L., *Geophys. J. R. astr. Soc.*, 7, 23-29 (1962a).
- 13 Van Zijl, J. S. V., Graham, K. W. T., and Hales, A. L., *Geophys. J. R. astr. Soc.*, 7, 169-182 (1962b).
- 14 Ito, H., and Fuller, M., *Palaeogeophysics* (Academic Press, London, 1970).
- 15 Ninkovitch, H. D., Opdyke, N. D., Heezen, B. C., and Foster, J., *Earth planet. Sci. Lett.*, 1, 476-492 (1966).
- 16 Dunn, J. R., Fuller, M., Ito, H., and Schmidt, V. A., *Science*, 172, 840-845 (1971).
- 17 York, D., Strangway, D. W., and Larson, E. E., *Earth planet. Sci. Lett.*, 11, 333-338 (1971).
- 18 Opdyke, N. D., Kent, D. V., and Lowrie, W., *Earth planet. Sci. Lett.*, 20, 315 (1973).
- 19 Prévot, M., and Watkins, N. D., *Annls Geophys.*, 25, 351-369 (1969).
- 20 Doell, R. R., and Cox, A., *Nature of the Solid Earth* (McGraw-Hill, New York, 1972).
- 21 Doell, R. R., *Geophys. J. R. astr. Soc.*, 26, 459-479 (1972).
- 22 Barbetti, M., and McElhinny, M., *Nature*, 239, 327-330 (1972).
- 23 Dagley, P., and Wilson, R. L., *Nature phys. Sci.*, 232, 16-19 (1971).
- 24 Lawley, E. A., *Earth planet. Sci. Lett.*, 10, 145-149 (1970).
- 25 Watkins, N. D., and Nougier, J., *J. Geophys. Res.*, 78, 6060-6068 (1973).

## Search for compression before a deep earthquake

DZIEWONSKI and Gilbert<sup>1</sup>, using a moment tensor representation of the seismic source, presented evidence for precursive compression before deep earthquakes. For the Colombian earthquake of July 31, 1970 (17:08:05.4 GMT, 1.5° S, 72.6° W,  $h > 650$  km), they concluded that a large precursive compression occurred in the focal region, beginning about 80 s before the origin times as determined by ordinary P wave travel times.

These results were, however, obtained from data derived from free oscillations with periods longer than 70 s, and so the time resolution is inevitably limited. Moreover, the phase information contained in the free oscillation data is somewhat obscured by the lateral heterogeneity of the Earth. It is therefore important to search for the existence of precursors by using an independent set of data. Thus, we have examined carefully the direct displacement field caused by a precursor. Specifically, we examined seismograms of the Colombian earthquake of July 31, 1970 and compared these observations with synthetic seismograms of the proposed precursor (Figs 1-4).

The epicentre of the July 31 earthquake is located relatively close to roughly a dozen World Wide Standard Seismograph Network (WWSSN) stations and also close to a station at Naña, Peru. The stations all lie between 6.07° and 16.0° from the epicentre. The wavelength of such a slow precursor is about 1,000 km, and so the Earth can be modelled by a homogeneous medium for our synthetic seismogram computations at these short distances.

For a contraction source with time function  $\chi(t)$ , the radial displacement in the medium is given<sup>2</sup> by;

$$u_r = \frac{M}{4\pi\rho\alpha^2} \frac{d}{dr} \left( \frac{1}{r} \chi(t-r/\alpha) \right) + \frac{-M}{4\pi\rho\alpha^2} \frac{1}{r^2} \left[ \chi(t-r/\alpha) + \frac{r}{\alpha} \chi'(t-r/\alpha) \right] \quad (1)$$

where  $\alpha$ =compressional velocity;  $\rho$ =density;  $r$ =radial distance; and  $M$ =moment of inertia.

The first and second terms in the brackets represent the near-field and far-field displacements, respectively. The time function

of the proposed precursor can be described adequately by the function:

$$\chi(t) = \begin{cases} 0 & t \leq -\tau_1 \\ \frac{1}{\tau_1 + \tau_2} [t + \frac{\tau_1}{\pi} \sin \frac{\pi}{\tau_1} t + \tau_1] & -\tau_1 \leq t \leq 0 \\ \frac{1}{\tau_1 + \tau_2} [t + \frac{\tau_1}{\pi} \sin \frac{\pi}{\tau_2} t - \tau] & 0 \leq t \leq \tau_2 \\ 1 & t > \tau_2 \end{cases} \quad (2)$$

where  $\tau_1$  is the precursor time constant,  $\tau_2$  the time constant of the post-seismic deformation, and  $t = 0$  refers to the 'origin time'. This time function avoids discontinuities in displacement, velocity and acceleration at both  $t = \tau_1$  and  $t = \tau_2$ , and represents one of the smoothest time functions for a given time constant. Substituting this time function into equation (1), doubling the result to account for the free surface effect, convolving it with the appropriate instrument functions, and including the necessary cosine factors to account for the azimuth and angle of incidence terms, we obtain the synthetic seismograms. In our present computation we used  $M = 5.0 \times 10^{27}$  dyne cm, the value suggested by Dziewonski and Gilbert<sup>1</sup>,  $\alpha = 8.5 \text{ km s}^{-1}$  and  $\rho = 3.5 \text{ g cm}^{-3}$  for the average upper

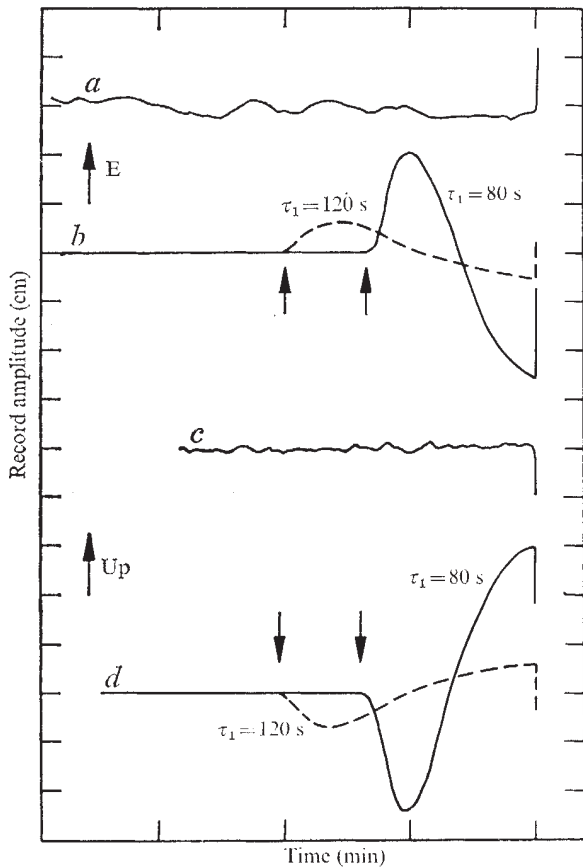


**Fig. 1** Long period, WWSSN seismogram from the QUI station (for July 31, 1970). E-W record: *a*, observed trace; *b*, synthetic trace. Vertical record: *c*, observed trace; *d*, synthetic trace. Arrows next to the synthetic traces (*b* and *d*) indicate precursor onsets. All traces end with the impulsive onset of the normal P wave. Peak magnification = 3,000;  $\Delta = 6.07^\circ$ .

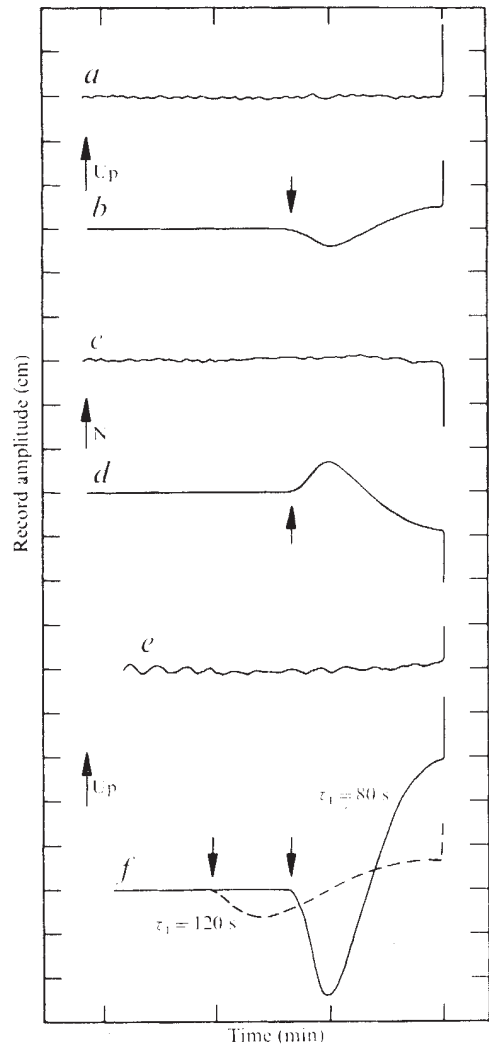


**Fig. 2** Long period WWSSN seismograms. *a-d*, ARE records: peak magnification = 1,500;  $\Delta = 14.94^\circ$ . Vertical: *a*, observed; *b*, synthetic. N-S: *c*, observed; *d*, synthetic. BOG records: peak magnification = 3,000;  $\Delta = 6.23^\circ$ ; *e*, observed; *f*, synthetic. Arrows next to the synthetic traces indicates precursor onsets.

mantle. For  $\tau_1$  and  $\tau_2$ , we consider three cases: (1)  $\tau_1 = \tau_2 = 80 \text{ s}$ , the value for the precursory time constant suggested in (the abstract of) Dziewonski and Gilbert<sup>1</sup>; (2)  $\tau_1 = 120 \text{ s}$ , and  $\tau_2 = 160 \text{ s}$ ; in this case,  $d\chi(t)/dt$  matches the isotropic moment rate tensor suggested by Dziewonski and Gilbert<sup>1</sup> (Fig. 5); and (3)  $\tau_1 = \tau_2 = 160 \text{ s}$ ; this last case represents a more gradual precursor which Dziewonski and Gilbert (personal communication) have suggested might be more appropriate (see Fig. 5).

Long period, vertical seismograms from five WWSSN stations—ARE, BOG, CAR, LPB, and QUI—were available to us. Long period, horizontal records from three of these stations—ARE, LPB, and QUI—were also examined. These seismograms and the corresponding synthetic seismograms are shown in Figs 1, 2, and 3. Recordings of the long period strain network and of the vertical pendulum seismometer at Naña, were also used in our investigations. These records and the respective synthetics are shown in Fig. 4. The very long period information on the strain record indicates tidal strains and some minor surface wave effects from an earlier earthquake in the South Pacific. Neither of these strains was included in the

synthetic strain record. The observed strain record has been fitted with a parabola for the 80 min preceding the onset of the main phase which closely approximates the tidal period. The synthetics for case (1) predict very large precursor amplitudes, as much as 6 cm peak to peak, on a WWSSN instrument operating at a peak magnification of 3,000. We were, however, unable to identify any trace of such an arrival on any of the

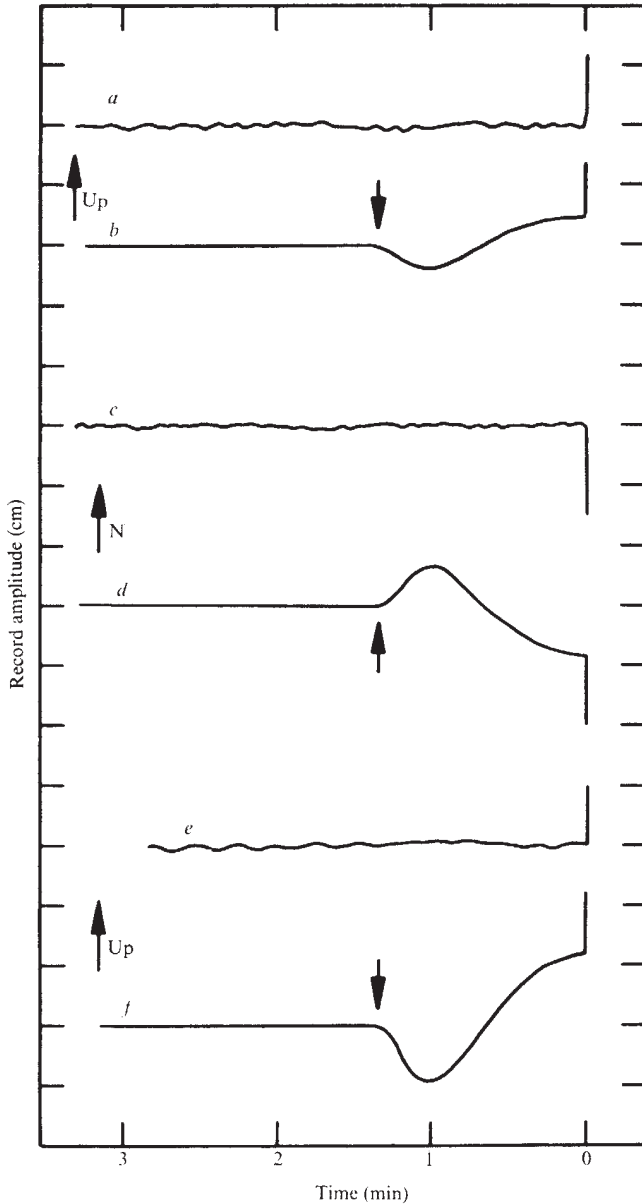


Fig. 3 Long period, WWSSN seismograms. *a-d*, LPB records: peak magnification—1,500;  $\Delta=15.61^\circ$ . Vertical: *a*, observed; *b*, synthetic. N-S: *c*, observed; *d*, synthetic. CAR records: Peak magnification=3,000;  $\Delta=13.15^\circ$ ; *e*, observed; *f*, synthetic. Arrows next to the synthetic traces indicate precursor onsets.

ten seismograms examined. Thus, if the precursor time constant is 80 s, the moment must be much less than that assumed here, probably less than  $5.0 \times 10^{26}$  dyne cm. For case (2), since the response curve for the Naña strain network is almost flat for  $T < 600$  s, the predicted amplitude is reduced only 30% from case (1) (Fig. 4A). In the case of the WWSSN instruments, however, we are dealing with the steep portion of the response

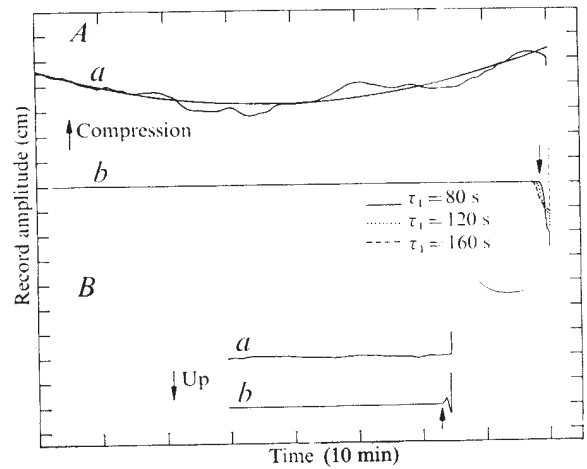


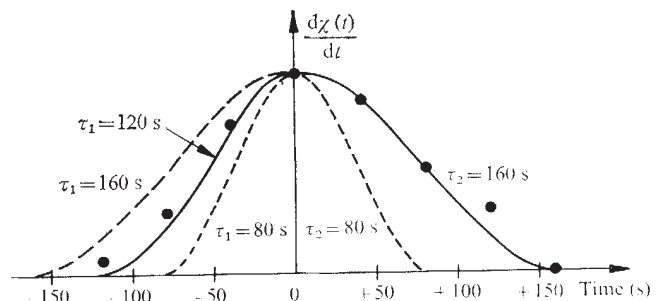
Fig. 4 *A*, Observed (*a*) and synthetic (*b*) strain records for the Caltech north-east strain network at Naña, Peru. Tidal effects removed from the synthetic. Small arrow indicates precursor onset;  $\Delta=11.21^\circ$ . Note the change of time scale between this figure and the preceding three. *B*, Observed (*a*) and synthetic (*b*) seismograms for Caltech vertical pendulum seismometer at Naña, Peru. Arrow indicates precursor onset;  $\Delta=11.21^\circ$ . Note that the polarity is reversed.

curve ( $\omega^3$ ) and the amplitude is greatly reduced by the increase in  $\tau_1$  from 80 to 120 s. Nevertheless, two nearby stations, QUI ( $\Delta = 6.07^\circ$ ) and BOG ( $\Delta = 6.23^\circ$ ), still show significant amplitudes (Figs 1 and 2). Thus, on the basis of Naña, QUI and BOG, we may conclude that the isotropic moment must be significantly smaller than the suggested value, probably less than  $10^{27}$  dyne cm. For case (3), the precursor signal is almost undetectable at all stations except Naña where the signal is still significant (Fig. 4A). If the precursory time is longer than about 200 s, the proposed isotropic precursor would be hardly detectable. This time constant is somewhat longer than that suggested by Dziewonski and Gilbert<sup>1</sup>, but in view of the discrete time interval of about 40 s used by them it might be within the permissible range.

We conclude that if the precursor time constant is less than 120 s, the isotropic moment must be less than  $10^{27}$  dyne cm or, if the precursor moment is  $5.0 \times 10^{27}$  dyne cm, the lower bound of the precursor time is 200 s.

One of us (R. S. H.) thanks the National Science Foundation for Graduate Fellowship support. We thank Professors Dziewonski and Gilbert for their comments on this manuscript.

Fig. 5 ●, Moment rate tensor ( $d\chi/dt$ ) data of Dziewonski and Gilbert<sup>1</sup>. The solid and dashed curves indicate the various moment rate tensors used in this study.



This research was supported by the Advanced Research Projects Agency of the Department of Defense and was monitored by the Air Force Office of Scientific Research.

ROBERT S. HART  
HIROO KANAMORI

Seismological Laboratory,  
California Institute of Technology,  
Pasadena, California 91109

Received June 10, 1974.

- <sup>1</sup> Dziewonski, A. M., and Gilbert, F., *Nature*, **247**, 185 (1974).  
<sup>2</sup> Love, A. E. H., *A Treatise on the Mathematical Theory of Elasticity*, 305 (Dover, New York, 1944).

DRS DZIEWONSKI AND GILBERT REPLY—We have stated that for two deep earthquakes the hypocentral region begins to experience compression about 80 s before the origin time determined from the first arrivals of P waves. This statement was based on an estimate of the time at which the isotropic moment rate begins to exceed the noise level visible in the deviatoric part of the moment rate tensor (Fig. 2 of ref. 1). The figure shows that isotropic moment rate is other than zero at times earlier than -80 s, and obviously our estimates of the "beginning" time could not have the meaning that Hart and Kanamori assigned to it.

Our measurements were carried out in the frequency domain. Transformation to the time domain required certain arbitrary, although clearly stated, assumptions because the spectrum was incomplete and contained noise. In these circumstances, if one attempts to introduce an analytical source function, the matching of the parameters should be done in the frequency domain. For the source function proposed by Hart and Kanamori<sup>2</sup> and the isotropic moment rate spectrum shown in Fig. 1 the best match is for a time constant of 160 s; a time constant of 200 s is also consistent with the data if  $M_0$  is allowed to increase by 50%. In either case the amplitudes of the synthetic seismograms would approach the noise level (the amplitudes would decrease by a factor comparable to that resulting from the increase of a time constant from 80 to 120 s).

It is disappointing that the result of the experiment by Hart and Kanamori is inconclusive, because it seems that with the present instrumentation it may be impossible to

confirm by observations in the time domain the occurrence of precursory phenomena such as those described in our paper<sup>1</sup>; the Colombian earthquake was the largest event in its depth range during the past 12 yr. Such confirmation would be very important, as at the present time we must rely on the assumption that the observed spectra should be smoothly interpolated to zero frequency. If this assumption were not valid, then compression might not be precursive. The most important result of our paper<sup>1</sup>, which is not subject to this assumption, is that there are volume changes associated with deep earthquakes and that their time function must be significantly different from that of the deviatoric (shear) moment tensor.

In the paper by Hart and Kanamori<sup>2</sup> we notice a long-period trend in the observed seismograms shown in Fig. 1a and c and Fig. 2c and e that agrees with the sign predicted by the theoretical calculations, that is, is consistent with the hypothesis of precursive compression. The same is true for a deflection on the strainmeter recording that occurred just before the earthquake. (The steeply rising pulse immediately following  $t = -\tau_1$  on the theoretical seismograms is determined by the properties of the source function at  $t = -\tau_1$ . This effect could be substantially reduced if Hart and Kanamori had chosen a function that has a more gradual rise.) Even though none of these examples is significant by itself, the fact that there are several of them is intriguing; particularly as there are no adverse cases.

- <sup>1</sup> Dziewonski, A. M., and Gilbert, F., *Nature*, **247**, 185 (1974).  
<sup>2</sup> Hart, R. S., and Kanamori, H., *Nature*, **253**, 333-336 (1975).

## Chemistry and origin of phlogopite megacrysts in kimberlite

STUDIES of the megacrysts occurring in kimberlite have hitherto neglected the mica megacrysts. We have analysed mica megacrysts from one Lesotho and twelve South African kimberlites. The megacrysts, which vary in size from 4 mm to 3 cm, were taken from both 'basaltic' and micaceous kimberlites, and distinguished from the matrix phlogopites by (i) their greater size; (ii) their dark brown, rather than bronze or light brown, colour; (iii) their rounded shape and corroded margins; (iv) distortion of the {001} planes (in some, but not all, megacrysts); and (v) absence of inclusions of matrix phases such as perovskite and spinel which often occur in the matrix micas.

The average and range of compositions of nine selected megacrysts are shown in Table 1, together with the averages of analyses for primary and secondary micas in peridotite xenoliths in kimberlite (ref. 1 and new data) and analyses of micas from four glimmerite nodules in kimberlite (three from the Bultfontein Mine, one from the Wesselton Mine). All the analyses were made by electron microprobe techniques, of which details will be given elsewhere. Nineteen megacrysts were analysed and checked for homogeneity at five or more points; the nine selected megacrysts were homogeneous, or nearly so, whereas the others showed variations of 5% or more in Fe. Inclusion of the other ten megacrysts does not affect the conclusions.

In Fig. 1, we plot  $\text{TiO}_2$  against  $\text{Cr}_2\text{O}_3$  for all our megacrysts and new data on micas from four peridotites, together with comparative data for ten peridotite micas given by Carswell<sup>1</sup>. Carswell had distinguished between primary and secondary micas in peridotites by virtue of lower  $\text{TiO}_2$ ,  $\text{Cr}_2\text{O}_3$ ,  $\text{Al}_2\text{O}_3$ ,  $\text{MgO}$  and  $\text{Na}_2\text{O}$ , but higher  $\text{SiO}_2$  in the primary micas. Our data for primary micas from peridotite fall very close to a field drawn from Carswell's analyses, whereas those for secondary micas extend towards higher  $\text{TiO}_2$  but maintain the high  $\text{Cr}_2\text{O}_3$  content. The same two oxides are shown for micas from the four glimmerite nodules. The lines AA' and

Fig. 1 Comparison of the observed moment rate spectrum with the spectra predicted by equation (2) of Hart and Kanamori<sup>2</sup> for several values of the time constant  $\tau$  ( $\tau = \tau_1 = \tau_2$ ).

